Comparative Transcriptome Analysis of Hypocotyls During the Developmental Transition of C_3 cotyledons to C_4 Leaves in *Halimocnemis mollissima* Bunge

Mahdis Zolfaghar[1], Twan Rutten[2], Mohammad Reza Ghaffari[*3], Ali Mohammad Banaei-Moghaddam[*1]

[1] Laboratory of Genomics and Epigenomics (LGE), Institute of Biochemistry and Biophysics, University of Tehran, Tehran, Iran

[2] Department of Physiology and Cell Biology, Leibniz Institute of Plant Genetics and Crop Plant Research (IPK), Stadt Seeland/OT Gatersleben, Germany

[3] Systems Biology Department, Agricultural Biotechnology Research Institute of Iran (ABRII), Agricultural Research, Education, and Extension Organization (AREEO), Karaj, Iran

[*] **Correspondence:**

Mohammad Reza Ghaffari

ghaffari@abrii.ac.ir (M.R.G)

Ali Mohammad Banaei-Moghaddam

am_banaei@ut.ac.ir (A.M.B-M)

ORCID ID:

Mahdis Zolfaghar 0000-0001-8762-3603

Twan Rutten 0000-0001-5891-6503

Mohammad Reza Ghaffari 0000-0002-7139-8613

Ali Mohammad Banaei-Moghaddam 0000-0003-1298-3748

Abstract

Identification of signaling pathways that control C_4 photosynthesis development is essential for introducing the C_4 pathway into C_3 crops. Species with dual photosynthesis in their life cycle are interesting models to study such regulatory mechanisms. The species used here *Halimocnemis mollissima* Bunge, belonging to the Caroxyleae tribe, displays C_3 photosynthesis in its cotyledons and a NAD-ME subtype of C_4 photosynthesis in the First leaves

(FLs) onwards. We explored the long-distance signaling pathways that are probably implicated in the shoot-root coordination associated with the manifestation of the C_4 traits, including efficient resource usage by comparing the mRNA content of hypocotyls before and after the C_4 first leave's formation. Histological examination showed the presence of C_3 anatomy in cotyledons and C_4 anatomy in the FLs. Our transcriptome analyses verified the performance of the NAD-ME subtype of C_4 in FLs and revealed differential transcript abundance of several potential mobile regulators and their associated receptors or transporters in two developmentally different hypocotyls of *H. mollissima* Bunge. These differentially expressed genes (DEGs) belong to diverse functional groups, including various transcription factor (TF) families, phytohormones metabolism, and signaling peptides, part of which could be related to hypocotyl development. Our findings support the higher nitrogen and water use efficiency associated with C_4 photosynthetic and provide insights into the coordinated above- and under-ground tissue communication during the developmental transition of C_3 to C_4 photosynthesis in this species.

Keywords: C_4 photosynthesis, *Halimocnemis mollissima* Bunge, long-distance signaling, NAD-ME subtype, RNA sequencing, Shoot-root coordination

Abbreviations

TF	Transcription factor
DEG	Differentially expressed gene
FLs	First leaves
PEPC	Phosphoenolpyruvate carboxylase
BCA	Beta-carbonic anhydrase
PPdK	pyruvate orthophosphate dikinase
Asp-AT	Aspartate aminotransferas
Ala-AT	Alanine aminotransferase
NAD-ME	NAD-dependent malic enzyme
NADP-ME	NADP-dependent malic enzyme
TPT	Triosephosphate translocator
PPase6	Pyrophosphatase
PPdK-RP1	Pyruvate orthophosphate dikinase related protein1
PPT2	PEP/phosphate translocator
BASS4	Bile acid:sodium symporter family protein
BASS2	Bile acid:sodium symporter family protein
AMK2	Adenosine monophosphate kinase
HY5	Elongated hypocotyl 5

57 SHR Short-Root

58

59 Introduction

60 As an adaptation to the hot and dry environment, C_4 photosynthesis is a carbon concentration mechanism that
61 reduces the counteracting photorespiration by suppressing the oxygenase activity of the carboxylating enzyme
62 RuBisCO (Ribulose-1,5-bisphosphate carboxylase/oxygenase). The leaves of C_4 plants have a unique structure
63 called Kranz anatomy, enabling them to spatially separate two phases of photosynthesis into the mesophyll and
64 bundle sheath cells. The Kranz anatomy precedes evolving C_4 biochemistry (McKown and Dengler 2007). A
65 universal feature of C_4 plants is their higher usage efficiency of resources such as nitrogen, water, and radiation
66 (Vogan and Sage 2011; Fatima *et al.* 2018). Nitrogen and water are uptaken by roots and are largely controlled
67 by the demands in the shoots. The indispensable shoot-root communication is coordinated by long-distance
68 signaling molecules such as phytohormones, signaling peptides, and TFs (Ko and Helariutta 2017).

69 Generally, in the C_4 pathway, the carbon fixation begins in the mesophyll, where carbon dioxide is
70 converted into bicarbonate and then to four-carbon (C_4) organic acids. The C_4 compounds are transported to the
71 bundle sheath and decarboxylated to release the CO_2 at the site of RuBisCO for assimilation (Sage 2004; Gowik
72 and Westhoff 2011). Based on the primary decarboxylating enzymes, NADP-ME and NAD-ME are two main
73 biochemical subtypes of the C_4 pathway (Rao and Dixon 2016). As a striking example of convergent evolution,
74 the conversion of C_3 into C_4 photosynthesis has evolved independently in more than 60 lineages of angiosperms
75 (Slewinski 2013). The polyphyletic origin of C_4 syndrome implies that the transition of C_3 into C_4 is not as
76 genetically complicated as inferred from the associated anatomical and biochemical features. It is suggested that
77 the pre-existing C_3 gene regulatory networks are recruited in the C_4 pathway with relatively few modifications
78 (Hibberd and Covshoff 2010; Reyna-Llorens and Hibberd 2017).

79 In addition to efforts distinguishing genes encoding C_4 enzymes, other studies have tried to identify the
80 genetic architecture and regulation of initiating the C_4 metabolism (Gowik *et al.* 2011; Wang, Vlad and Langdale
81 2016; Cui, 2021). For this transcriptome profiles were compared of C_3 and C_4 tissues of close relative (C_3 and C_4
82 *Flaveria*) (Gowik *et al.* 2011) or distantly related (C_3 rice and C_4 maize) (Wang *et al.* 2014) species. Most of the
83 omic analyses on C_4 photosynthesis have been performed in C_4 plants belonging to the NADP-ME subtype (Gowik
84 *et al.* 2011; Lauterbach *et al.* 2017). However, to comprehend the nature and commonality of regulatory features
85 of C_4 syndrome it is essential to investigate both biochemical subtypes. The nature and mechanism of distant

86 signaling molecules act in C_4 plants to coordinate the above- and under-ground tissues to maintain their
87 homeostasis and establish C_4 features, including Kranz anatomy, nitrogen, and water use efficiency, remains
88 largely obscure and has hampered the long-standing goal of engineering C_4 metabolism into the C_3 crops (Gerlich
89 *et al.* 2018).

90 Recently, species such as *Haloxylon ammodendron* (Y. Li *et al.* 2015) and *Salsola soda* (Lauterbach,
91 Billakurthi et al. 2017) have been found to display two photosynthetic mechanisms in their life cycle. As such
92 they provide an excellent model for studying the molecular regulatory mechanisms underlying the coordination
93 of roots and modified shoots during the C_3 to C_4 conversion while eliminating phylogenetic noises that hindered
94 earlier models. Unlike the C_3 pathway in cotyledons, which coincides with moderate temperature, the C_4 pathway
95 in these plants, which belongs to the NADP-ME subtype of C_4 photosynthesis, outperforms at higher light and
96 temperature conditions concurrent with the formation of the first leaf stage onwards (Lauterbach, Billakurthi et
97 al. 2017).

98 *H. mollissima* Bunge used in the present study belongs to the Caroxyleae tribe and performs both C_3 (in
99 cotyledons) and C_4 photosynthesis (NAD-ME subtype, in FLs onwards) (Akhani *et al.* 2009). To unravel the
100 signaling pathways associated with the C_3 to C_4 transition in *H. mollissima* Bunge, we used RNA sequencing to
101 generate transcriptome profiles of hypocotyls before and after forming the C_4 FLs alongside the FLs. Genes
102 associated with several phytohormone metabolisms, TFs, and signal peptides were differentially expressed in
103 hypocotyls before and after forming C_4 FLs. Our results indicated that, besides those associated with hypocotyl
104 development, some of these genes show homology to known shoot-to-root and vice-versa signals and their
105 receptors or transporters that are possibly implicated in establishing unique C_4 traits, especially in the efficient
106 consumption of resources such as nitrogen and water.

107 Material and Methods

108 Plant Cultivation and Sampling

109 Seeds of *H. mollissima* Bunge were collected at Mahdasht, Karaj, Iran ($35^{o}43'^{35.4}$"N; $50^{o}44'04.5$"E) in November
110 2019 and stored at 4^{oC}. After removal of the hard seed coats, seeds were disinfected with ethanol 75%, washed
111 with water and germinated on the wet, sterilized filter paper in Petri dishes. After root formation, at 3 days after
112 incubation (DAI), seedlings were transferred into the plastic pots (5 cm diameter, 7 cm height) filled with sand,

113 perlite, and compost. *H. mollissima* Bunge Plants were grown in a greenhouse at the Institute of Biochemistry and
114 Biophysics, University of Tehran, at 25-30^{oC}, ~200 µmol m^{-2} s^{-1} illumination and 16/8-hours light/dark cycle.

115 For sampling, two series of *H. mollissima* Bunge were cultivated. In the first series, expanded cotyledons,
116 hypocotyls, and roots (Series A) (Fig. 1(a)) were harvested before FLs were formed. In the second series, FLs,
117 cotyledons, hypocotyls, and roots (Series B) (Fig. 1(b)) were harvested after formation of FLs. Tissues of interest
118 were sampled in January and February 2020 between 11:00 and 13:00, shock-frozen in liquid nitrogen and stored
119 at -80^{oC}. Two biological replicates of hypocotyls and FLs and three of all sampled tissues were used for RNA
120 sequencing and RT-qPCR, respectively, each containing pooled tissue from 5 independent plants.

121 **Light Microscopy**

122 For histological studies, C_3 cotyledon and C_4 first leaf were fixated for 16h in 50 mM Phosphate Puffer, pH 7.0,
123 containing 1 % (v/v) glutaraldehyde and 4 % (v/v) formaldehyde at 8°C. After 2 x 10 min washing with distilled
124 water and subsequent dehydration in an ascending ethanol series (30, 40, 50, 60, 75, 90 % and 2 × 100 % ethanol,
125 10 min each), probes were infiltrated with Spurr resin and polymerized in an oven at 70°C for 24 h. Semithin
126 sections of the middle regions of fully expanded cotyledons and FLs were made on a Reichert Ultracut S (Leica
127 Microsystems, Wetzlar, Germany) and stained with 1 % (w/v) methylene blue and 1 % (w/v) Azur II. Images
128 were taken on a Zeiss Axiovert 135 microscope (Carl Zeiss, Jena, Germany) and stored as TIFF files.

129 **RNA Extraction and Sequencing**

130 The guanidine/ phenol-based method (Chomczynski and Sacchi 1987) was used to isolate total RNA from 100-
131 150 mg of the homogenized samples. Quality, quantity, and integrity of isolated RNA were checked by Agarose
132 gel electrophoresis, Nanodrop (Thermo Fisher Scientific), and Agilent Bioanalyzer 2100 system (Agilent
133 Technologies Co. Ltd., Beijing, China), respectively. High-quality RNA (RIN value > 5.2) was used for cDNA
134 preparation and sequencing by Illumina Hiseq 2500 platform at the Novogene Bioinformatics Institute (Beijing,
135 China). One hundred fifty bp paired-end reads were obtained, and their adapter-contained and low-quality
136 (Qscore< = 5) base-contained were removed.

137 **De novo Assembly and Functional Annotation**

138 Raw reads were evaluated for quality by FastQC tool
139 (http://www.bioinformatics.babraham.ac.uk/projects/fastqc/). Due to removing adapters and low-quality reads by

140 the Novogene Bioinformatics Institute, there was no need for trimming. High-quality reads were assembled by
141 Trinity v2.4.0 (Grabherr *et al.* 2011) using default settings. First, probable open reading frames (ORF) were
142 predicted using the Transdecoder tool (Haas and Papanicolaou, 2016) with a minimum length of 100 amino acids.
143 To obtain Gene Ontology (GO) terms of the transcripts, Blast2GO software was used with $1e^3$ as an e-value cut-
144 off to perform BlastX against a non-redundant protein database. The online KEGG Automatic Annotation Server
145 (KAAS) (http://www.genome.jp/kegg/kaas) and Mapman V4.0 (https://www.plabipd.de/portal/mercator4)
146 (Schwacke *et al.* 2019) were used for pathway analysis (p-value ≤ 0.05). Also, the Arabidopsis TAIR locus IDs
147 were assigned to each transcript during Mapman analysis (https://www.plabipd.de/portal/web/guest/mercator-
148 sequence-annotation) (Lohse *et al.* 2014).

149 **Determination of Genes with Different Expression**

150 RSEM tool (http://deweylab.biostat.wisc.edu/RSEM) (Li and Dewey 2011) was used to estimate the abundance
151 of the transcripts for each sample. The high-quality raw reads were separately mapped back onto the assembled
152 transcripts using Bowtie 2.0. Differential expression analysis was performed by edgeR (Robinson, McCarthy and
153 Smyth 2010) in R after normalization using the trimmed mean of M-values (TMM) method. Statistical tests for
154 the pairwise comparisons were Benjamini-Hochberg correction FDR ≤ 0.05, $\log_2$FC ≥ 1.5 or ≤ -1.5 to set a
155 significant threshold for determining DEGs. Principal component analysis (PCA) with $\log_2$ transformed read count
156 (Transcript Per Million TPM) was performed in RStudio to visualize the expression pattern of the samples.
157 Furthermore, hierarchical clustering of the transcript abundance of selected known C_4 proteins using Pearson
158 correlation, average linkage method was performed (http://www.heatmapper.ca/expression/).

159 The DEGs most likely associated with the hypocotyl development of *H. mollissima* Bunge were excluded
160 from further analysis by comparing them with DEGs involved in the hypocotyl development in other plants of
161 flax and hemp (Roach and Deyholos 2008; Behr *et al.* 2018)
162 (https://bioinformatics.psb.ugent.be/webtools/Venn/).

163 **Determination of Active Biological Functions**

164 Pathways in each tissue of interest were explored using the percentage of total transcripts (normalized to
165 Transcript Per Million (TPM)) of each particular bincode in Mapman V4.0. According to the further emphasis of
166 this study on the survey of probable long-distance signaling, gene enrichment analysis was conducted by PageMan
167 software (Usadel *et al.* 2006) through Fisher's exact test followed by the Benjamini-Hochberg correction to

168 identify significant differences of Mapman bins among the two developmentally different hypocotyls. Moreover,
169 Mapman V3.6.0RC1 was used to visualize selected DEGs (through the generation of a custom MapMan pathway
170 image) encoding phytohormone synthesizing and degrading enzymes, transporter ("Phytohormone action bin"
171 and "Solute transporter"), and also genes related to different signal transduction pathways ("Multi-process
172 regulation. Calcium-dependent signaling", "Protein modification. Protein kinase" and "Redox homeostasis" bins).

173 **Identification of TFs and Prediction of Cis-acting elements in the Promoter of Predicted Mobile**
174 **TFs**

175 To predict differentially expressed TFs between hypocotyl before and after the formation of the FLs, the homology
176 of related amino acid sequences against the plant TFs database (PlantTFDB V5.0, http://planttfdb.gao-
177 lab.org/prediction.php) was implemented. Afterward, TFs with mobile mRNA, based on the information about
178 the genes with "cell-to-cell mobile mRNA" in The Arabidopsis Information Resource (TAIR) database, were
179 predicted.

180 Since the *H. mollissima* Bunge genome is not yet available, the promoter region of the orthologs of
181 predicted mobile TFs in Arabidopsis was obtained from the Arabidopsis Gene Regulatory Information Server
182 (AGRIS) database (https://agris-knowledgebase.org/AtcisDB/), and their cis-acting were predicted using
183 PlantCARE (http://bioinformatics.psb.ugent.be/webtools/plantcare/html/).

184 **Real-time quantitative PCR (RT-qPCR)**

185 To confirm RNA seq data, RT-qPCR was performed for eight genes. Total RNA was extracted by the above-
186 mentioned method (Chomczynski and Sacchi, 1987) and treated with DNase I (Thermo Fisher). RNA was reverse
187 transcribed with the AddScript cDNA Synthesis Kit (add bio), according to manufacturer's instructions, using 1
188 µg of RNA. RT-qPCR was performed with a 6plex real-time PCR system (Qiagen, Rotor Gen Q, Germany) using
189 the RealQ Plus 2x Master Mix Green kit, without ROX (AMPLIQON) using 1 µL of 1:40-fold diluted template
190 cDNAs. Run conditions were: 10 min of initial denaturation at 95°C, 95°C for 30s, 60°C for 30s, and 72°C for
191 30s (40 cycles). Melting curve analysis and agarose gel electrophoresis were done to verify the primer specificity.
192 Primer efficiency was estimated for each primer pair by four consecutive 10-fold dilutions of the cDNAs as a
193 template. The relative expression of genes was calculated using the $2^{-\Delta\Delta Ct}$ method (Livak and Schmittgen 2001)
194 using the Polyubiquitin ortholog from *H. mollissima* Bunge as an endogenous control. Three biological replicates
195 were quantified for each sample.

196 **Results**

197 **Cotyledons and FLs of** *H. mollissima* Bunge **have Different Anatomical Features in Accordance**
198 **with Their Photosynthesis Strategy**

199 C_3 cotyledons of *H. mollissima* Bunge are flattened, bifacial, and their cross-section (Fig. 2 (a)) doesn't show any
200 Kranz anatomy. They have several layers of chlorenchyma cells around the vascular bundles (VBs) and
201 intercellular airspaces across the blades (Fig. 2 (a)). While C_4 first leaf is terete, linear, and covered by hairs, and
202 its anatomy is salsoloid. The leaf cross section (Fig. 2 (b) and (c)) shows a large central water storage tissue which
203 is respectively surrounded by the Kranz layer, palisade mesophyll cells, and a single-layered epidermis, while
204 there is no space to be seen in the microscopic leaf structure.

205 **Processing of Raw Reads and Statistics of De novo Assembly**

206 The mRNA of three different tissues, including hypocotyls before (hypocotyl A) and after (hypocotyl B) the
207 formation of FLs, and the FLs themselves (FL), were sequenced. The quality of reads was checked, and based on
208 FastQC results (Phred score= 36) all reads had high quality (Additional file 1(A)) circumventing the need for
209 further trimming. Raw data is available in the ? database under accession number ? (Additional file 2). To evaluate
210 the Trinity results, N50 and total assembly length were checked by Trinitystat.pl (Additional file 1 (B)). PCA
211 analysis (Fig. 3), where the first principal component contained 69.57% and the second principal component had
212 21.52% of the variance, demonstrated that the analyzed tissues have a distinct expression patterns. Nevertheless,
213 the replicates' expression data were similar and grouped. As expected, the same tissues (hypocotyl A and
214 hypocotyl B) had more similar expression patterns than the FLs.

215 **Determination of Active Functional Pathways in analyzed tissues**

216 To evaluate how the transcriptome as whole changes during the transition of photosynthesis strategy, the
217 functional classes of each tissue transcriptome were determined as the percentage of all transcripts (normalized to
218 Transcript Per Million (TPM)) assigned to each Mapman bincodes (Fig. 4(a), Additional file 3). MapMan analysis
219 showed "Not assigned, annotated" and "Not assigned, not annotated" with 19.41 and 45.86% of all transcripts
220 being the most significant functional gene categories in each sample. While with 15.44% the "Photosynthesis"
221 bin was the third-highest abundant functional class in the FLs, in the hypocotyl A and B it accounted for only
222 3.25% and 2.47%, respectively. Out of 16 transcripts associated with known C_4 proteins, 14 transcripts, including
223 Beta-carbonic anhydrase (BCA3), PEP carboxylase1 (PEPC1), pyruvate orthophosphate dikinase (PPdK),

224 aspartate aminotransferase (Asp-AT), alanine aminotransferase (Ala-AT), NAD-dependent malic enzyme (NAD-
225 ME), NADP-dependent malic enzyme (NADP-ME), Triosephosphate translocator (TPT), Pyrophosphatase
226 (PPase6), pyruvate orthophosphate dikinase related protein1 (PPdK-RP1), PEP/phosphate translocator (PPT2),
227 Bile acid:sodium symporter family protein (BASS4), Bile acid:sodium symporter family protein (BASS2),
228 Adenosine monophosphate kinase (AMK2) were more abundant in FLs than hypocotyls (Fig. 4(b), Additional
229 file 4). As expected, NAD-ME is more abundant than NADP-ME in FLs.

230 "Protein biosynthesis" and "Protein homeostasis" were the third- and fourth-highest abundant functional
231 categories in hypocotyl A (4.68 and 3.96%, respectively) and B (4.67 and 4%, respectively) (Fig. 4(a)). "RNA
232 biosynthesis" (1.92-2.34%) and "solute transport" (1.87-2.09%) were also abundant in all three samples
233 (Additional file 3). Although the abundance of most functional categories is similar in hypocotyl A and B, the
234 "RNA biosynthesis" (2.04 and 2.34 %, respectively) and "Phytohormone action" (1.2 and 1.31%, respectively)
235 classes are somewhat more abundant in the hypocotyl B.

236 The Pairwise comparison between the samples revealed several DEGs (FDR<= 0.05) among three
237 different developmental tissues (Additional file 5). In order to identify possible signaling pathways involved in
238 the C_3 to C_4 transition, pathways enrichment analysis was conducted for 8424 DEGs in the hypocotyl B vs.
239 hypocotyl A comparison. Among the pathways that according to the overrepresentation analysis appeared to be
240 up-regulatedly enriched in hypocotyl B were those involved in "Protein biosynthesis", "Protein homeostasis and
241 the ubiquitin-proteasome system" (Fig. 5).

242 Next, to explore possible long-distance regulators, we focus on the various regulatory mechanisms by
243 further analyzing DEGs in the two developmentally different hypocotyls. To differentiate between genes
244 controlling the transition of photosynthesis strategy and those involved in hypocotyl development, we compared
245 them (based on the assigned Arabidopsis IDs) with previously identified genes associated with hypocotyls
246 development (Roach and Deyholos, 2008; Behr *et al.* 2018). This way 190 genes were excluded (Additional file
247 6, Additional file 7). We then focused on the unique genes which do not overlap with related developmental genes.

248 **DEGs Associated with Classical Phytohormones Metabolism**

249 Mapping of unique DEGs of hypocotyl B vs. hypocotyl A in Mapman V3.6.0RC1 (Fig. 6, Additional file 8)
250 indicated several genes involved in the biosynthesis, degradation, transport, and signal transduction of plant
251 hormones (Phytohormone bin in Mapman) that are up- or down-regulated after the establishment of C_4
252 photosynthesis in the FLs.

253 Several transcripts encoding membrane bound auxin transporters, such as PIN-FORMED (PIN) (PIN2;
254 At5g57090), and membrane-bound ATP-binding cassette-B (ABCB) auxin transporter (ABCB19; At3g28860),
255 which are involved in long-distance auxin signaling proved to be less abundant in hypocotyl B compared to
256 hypocotyl A. Other auxin-responsive genes like NITRATE TRANSPORTER 1 (NRT1; AT1G12110), an auxin-
257 responsive transporter, were down-regulated in hypocotyl B after C_4 establishment, as was the flavin-dependent
258 monooxygenase (YUCCA) involved in auxin biosynthesis. In contrast, transcripts of several PIN-Like
259 transporters (PILS), which are distributed in the intracellular compartments and mediate intracellular auxin
260 homeostasis, were more abundant in hypocotyl B. Also transcripts assigned to AUX/ IAA (AT5G43700,
261 AT3G04730, and AT4G29080) and ARF7/ARF19 (AT1G19220) auxin signal transduction genes were up-
262 regulated in hypocotyl B. Apparently, the biosynthesis and long-distance transport of auxin are reduced in
263 hypocotyls after the formation of the FLs. In contrast to this, almost all transcripts associated with different
264 cytokinin pathways bin (biosynthesis, signaling and transport) were up-regulated in hypocotyl B (Fig. 6). For
265 example, type-B ARABIDOPSIS RESPONSE REGULATOR (ARR) and type-A ARR, involved in the cytokinin
266 signaling, were up- and down-regulated in the hypocotyl B, respectively. Also, transcripts of ENT
267 (EQUILIBRATIVE NUCLEOTIDE TRANSPORTER 1) (at4g05120, at1g70330), importers to take up apoplastic
268 nucleosides of cytokinins, were more expressed in the hypocotyl B. DEGs associated with brassinosteroids were
269 down-regulated.

270 Several long-range hormone transporters were more expressed in hypocotyl B (Fig. 6, Additional file 8),
271 such as ABCG30 (AT4G15230), ABCG40 (AT1G15520), LHT1 (LYSINE-HISTIDINE TRANSPORTER)
272 (at5g40780). NPF3.1 (Nitrate transport1/Peptide transporter family) (at1g68570), which is a multihormone
273 transporter involved in the GA/ABA antagonism (Hirner *et al.* 2006), was down-regulated in hypocotyl B.

274 **Differentially Expressed Signaling Peptides**

275 Overrepresentation analysis of DEGs in hypocotyls before and after the formation of the FLs revealed that in
276 contrast to the CRP classes of plant peptides (showing an overrepresentation of down-regulated genes), transcripts
277 related to NCRP did not show enrichment in hypocotyls after the formation of the FLs (Fig. 5). Transcript
278 abundance of different groups of these classes, based on Mapman bins, was then compared between analyzed
279 tissues which showed a complex pattern of up and down-regulation (Fig. 7, Additional file 4). In general,
280 transcripts belonging to different groups of the CRP categories were less abundant in hypocotyls after the
281 establishment of C_4 photosynthesis in the FLs (Fig. 7 (a)). In this regard, transcripts assigned to several GASA

282 group members, including GASA1 (at1g74670), GASA8 (AT2G39540), GASA13 (AT3G10185), GASA14
283 (AT5G14920), and GASA 10 (AT5G59845) as well as RALF signaling peptides like RALF33 (AT4G15800) and
284 its receptor CrRLK1L were down-regulated in hypocotyl after C_4 manifestation. Transcripts encoding peptides
285 belonging to NCRP classes, including plant natriuretic peptide (PNP), CLAVATA3-EMBRYO-
286 SURROUNDING REGION (CLE), Casparian strip integrity factor (CIF), PAMP-INDUCED SECRETED
287 PEPTIDE (PIP) were more abundant in the hypocotyl after the formation of FLs (Fig. 6, Fig. 7 (b)). However,
288 transcripts that are assigned to the receptor of C-terminally Encoded Peptides (CEP) such as CEPR2
289 (AT1G72180), acting in the nitrogen uptake signaling and Root meristem growth factor, were down-regulated in
290 the hypocotyl after FLs formation.

291 **DEGs Taken Part in Various Signal Transduction Pathways**

292 The binding of the ligands to their receptors at the cell surface triggers intracellular reaction cascades to amplify
293 the input signals, eventually altering gene expression in various pathways. We found that transcripts of genes
294 involved in the transduction pathways were differentially regulated in the hypocotyls after forming the FLs (Fig.
295 6). Transcripts of several protein kinase genes belonging to the casein kinase (CK) and sterility (STE) protein
296 kinase superfamilies, which are implicated in responses to many signals, were more abundant in hypocotyl after
297 forming the FLs. Most genes belonging to the AGC (PKA-PKG-PKC), and CMGC (Cyclin-dependent kinases,
298 Mitogen-activated protein kinases (MAPK), Glycogen synthase kinases, and Cyclin-dependent like kinases)
299 superfamilies were more expressed in hypocotyl B, as were transcripts associated with receptor-like cytoplasmic
300 protein kinases (RLCKs).

301 Also several genes involved in redox signaling and also those encoding for calmodulin-like proteins
302 (CMLs) involved in plants Ca2+ signaling processes were up-regulated in the hypocotyl after the formation of the
303 FLs (Fig. 6).

304 **Differentially Expressed TFs**

305 According to PlantTFDB V5.0, 290 out of 9640 ORFs from differentially expressed transcripts between hypocotyl
306 before and after the formation of the FLs were annotated as different TF families with the best fit in *A. thaliana*
307 locus IDs (Additional file 9). The mRNA levels of 71 and 219 of these TFs were down- and up-regulated,
308 respectively, in hypocotyl after the formation of the FLs. In this comparison, C2H2, bHLH, and NAC families
309 had a larger number of differentially regulated transcripts. Almost all transcripts belonging to C2H2, C3H, GRAS,

310 MYB, TCP, Trihelix, NF-Y, and WRKY TFs had more expression in hypocotyl after the formation of the FLs.
311 SHORT ROOT (SHR) (AT4G37650), a member of the GRAS family, and ELONGATED HYPOCOTYL 5
312 (HY5) (AT5G11260, AT3G17609), a member of the basic leucine zipper (bZIP) family, were up-regulated in
313 hypocotyl after the formation of the FLs. Notably, both SHR and HY5 are shown to have mobility and could
314 affect the expression of other genes (Dolan 2001; Chen *et al.* 2016).

315 Among 290 differentially expressed transcripts that were annotated as TFs based on PlantTFDB, 12 of
316 them had orthologous with cell-to-cell mobile mRNA, according to the TAIR database (Table 1). Eight of these
317 TFs were more abundant in hypocotyl after the formation of the FLs, including SCL1 (GRAS family,
318 AT1G21450), HAT22 (HD-ZIP family, AT4G37790), HSFA1E (HSF family, AT3G02990), CDC5
319 (MYB_related, AT1G09770), MYBH (MYB_related family, AT5G47390), NAC053 (NAC family,
320 AT3G10500), NAP (NAC family, AT1G69490) and ATWRKY40 (WRKY family, AT1G808$_4$0).

321 To predict if specific cis-regulatory elements are overrepresented in the regulatory region of candidate
322 mobile TFs with differentially expression levels in hypocotyls, PlantCARE (Lescot *et al.* 2002) was used to
323 analyze the upstream promoter elements of the Arabidopsis orthologs of these transcripts. The results showed that
324 Arabidopsis orthologs of differentially regulated mobile TFs carry several different cis-elements responsive to
325 phytohormones and environmental stimuli such as light and temperature. Among these, Box 4 (part of a conserved
326 DNA module involved in light responsiveness), AE-box (part of a module for light response), G-Box (cis-acting
327 regulatory element involved in light responsiveness), and GT1-motif (light-responsive element) were more
328 common light-responsive elements in the upstream of the mobile TFs (Additional file 10). Besides, the ABA-
329 responsive element (ABRE) was predicted in the promoter of BOA, SCL1, HAT22, MYBH, NAC053, ATAF1,
330 NAP, and WRKY40 TFs. Other motifs related to stress responses, including the MYB binding site involved in
331 drought-inducibility (MBS), a cis-acting element involved in defense and stress responsiveness (TC-rich repeat),
332 and a cis-acting regulatory element involved in the MeJA-responsiveness (CGTCA-motif and TGACG-motif),
333 were predicted to be present in the upstream region of the orthologs of differentially regulated mobile TFs genes
334 after the formation of the FLs.

335 To confirm RNA sequencing results, RT-qPCR was performed for eight target genes. The results were
336 correlated with the RNA seq analysis (R^2=0.81; Additional file 11). The RT-qPCR data analysis confirmed a
337 higher abundance of the C_4 enzymes, PEPC, BCA, and NAD-ME encoding genes in the FLs compared to the
338 cotyledons (Fig. 8(a)). The expression pattern of the analyzed genes somewhat varied between developmentally

339 different cotyledons and hypocotyls (Fig. 8(b), 8(d)). PEPC, BCA, NAD-ME, CEPR2, AUX/ IAA, ABCG40,
340 WRKY40, and NRT1.1 were less expressed in the roots after the formation of the FLs (Fig. 8(c)).

341 **Discussion**

342 **Species with Switching Mechanisms are Valuable Models for studying C_4 Photosynthesis**

343 We investigated the transcriptome profile of *H. mollissima* Bunge hypocotyls before and after first leaf formation
344 to identify possible components of long-distance signaling pathways involved in the unique C_4 traits through the
345 connection between the above- and under-ground tissues. *H. mollissima* Bunge belongs to the Caroxyleae tribe
346 and has two photosynthetic mechanisms in its annual life cycle; C_3 in cotyledons and NAD-ME subtype of C_4 in
347 the FLs onwards. Anatomical studies of cotyledons and FLs (Fig. 2) reveal features related to C_3 and C_4
348 (Salsoloid) (Akhani *et al.* 2009; Freitag and Kadereit 2014), respectively. In leaves the proportion of water storage
349 tissue was larger compared to the cotyledons while air space volume was less. This correlates with the
350 development of functional and efficient C_4 photosynthesis. Akhani et al. (Akhani *et al.* 2009) who determined the
351 carbon isotope composition of cotyledons and leaves of *H. mollissima* Bunge, found that cotyledons and leaves
352 have C_3 and C_4 type isotope values, respectively. This fits with our observations of typical C_4 genes (PEPC, BCA,
353 and NAD-ME) being higher expressed in the FLs (Fig. 8(A)).

354 A C_3 to C_4 switching mechanism has been reported for several species in the Salsoloideae (Caroxyleae
355 and Salsoleae tribes) and Suadedoideae subfamilies (Rudov *et al.* 2020). Thus, their germination usually coincides
356 with low-temperature conditions that possibly favor C_3 photosynthesis in the cotyledons. As these species grow
357 and the temperature rises, C_4 photosynthesis is encouraged in the leaves (Rudov *et al.* 2020). Plants expressing
358 such C_3 to C_4 switching may be appropriate models to explore the C_4 pathway and its regulatory mechanisms due
359 their lack of phylogenetic noises and interspecies differences. Transcriptome analysis of *Haloxylon ammodendron*
360 (Y. Li *et al.* 2015) and *Salsola soda* (Lauterbach, Billakurthi et al. 2017) both belonging to the *Salsoleae* tribe and
361 performing a NADP-ME subtype of C_4 photosynthesis in true leaves, revealed differentially expressed C_4 pathway
362 genes, such as PEPC between C_3 cotyledons and C_4 true leaves, but paid less attention to possible differences in
363 regulatory pathways. In the present study we investigated potential shoot-root communications during the C_3 to
364 NAD-ME subtype of C_4 transition by focusing on the DEGs in hypocotyls before and after the C_4 first leave's
365 formation.

366 **Novel Consistent Data Provided by *De novo* Assembly of** *H. mollissima* Bunge **Transcriptome**

367 Most transcriptome data analyses in the field of C_4 photosynthesis, with a few exceptions, have used a reference-
368 based approach to annotate their data using the Arabidopsis data (Gowik and Westhoff 2011; Lauterbach,
369 Billakurthi *et al.* 2017; Lauterbach, Schmidt *et al.* 2017; Siadjeu, Lauterbach and Kadereit 2021). As a non-model
370 species from the Caroxyleae tribe whose genome is not sequenced, we used RNA-seq to de novo assemble and
371 characterize the *H. mollissima* Bunge hypocotyls and FLs transcriptome.

372 PCA (Fig. 3) and analysis of functional classes of annotated genes (Fig. 4(a)) confirm the sequencing
373 data's reasonable and comparable relationship. Based on functional annotation, FLs expressed the NAD-ME
374 subtype of the C_4 photosynthesis pathway. The expression of photosynthesis-related genes was reduced in
375 hypocotyls after establishing the photosynthetic leaves. The formation of FLs also coincides with increased
376 translation processes in the hypocotyls an example of this being the upregulation of the ubiquitin-proteasome
377 system, a critical regulator of many plants signaling pathways in respond to internal and external cues
378 (Sadanandom *et al.* 2012).

379 Possible Regulatory Mechanisms Implicated in the Unique C_4 Features through Adjustment of 380 Shoot and Root Communication

381 Several regulatory systems with overlapping functions control the developmental processes in plants. These
382 include among others phytohormones, signaling peptides, and complex network of TFs. Long-range regulators
383 are an essential part of these systems. C_4 photosynthesis which is seen as a response to a reduced atmospheric
384 CO_2, requires a coordination between the root and the modified shoot. Similarly, the onset of the C_4 pathway in
385 leaves, followed by increased photosynthesis rate and more efficient use of resources, requires coordination
386 between roots and the modified shoots via signaling molecules. Interspecies grafting experiments between C_3
387 *Flaveria robusta* and C_4 *Flaveria bidentis* indicated that the root preliminary controls sulfur allocation between
388 roots and shoots and sulfur homeostasis in C_4 *Flaveria* (Gerlich *et al.* 2018). The communication ways between
389 above- and below-ground plant parts are very diverse. They can be physical (e.g. propagating Ca^{2+} waves),
390 chemical (e.g. signaling peptides and hormones), or molecular (e.g. RNA and proteins) (Shabala *et al.* 2015).
391 These signals can move through vasculature systems or cell-by-cell via stems or stem-like tissue (Bartusch and
392 Melnyk 2020). Also, the phloem comprises several mobile developmental signals (mRNAs, proteins, peptides,
393 e.g.), which can interplay in the different stages of development and growth (Koenig and Hoffmann-Benning
394 2020). Long-range movement of regulatory molecules has already been demonstrated, for auxin (Bellstaedt *et al.*
395 2019), cytokinin, abscisic acid (Kiba *et al.* 2011), various signaling peptides such as CEP, specific transporters or

396 receptors and some TFs (Shabala *et al.* 2015). By comparing transcriptome profiles of hypocotyls during the C_3
397 to C_4 transition, we revealed that transcripts of genes encoding components of different phytohormone
398 metabolisms, signaling peptides, and TFs (Fig. 6, Additional file 8) were differentially expressed in hypocotyls
399 after establishing the C_4 leaves. In addition, the expression levels of several transporters, receptors, and responsive
400 genes of root- or leaf-derived signals were also affected, including those of PIN1, CEPR, and ARF7/ARF19 (Fig.
401 6, Additional file 8). Some of these regulators are most likely implicated in the normal development of hypocotyls.
402 Therefore, to distinguish true C_4-related genes, we used a literature survey to exclude those genes involved in the
403 hypocotyl development (Additional file 6, Additional file 7). The mobility of mRNA as long-distance signal is
404 supposed to be a complex process while elucidating its physiological roles remains challenging (Xia *et al.* 2018).

405 Nitrogen Use Efficiency: The Reduction of Shoot-to-Root Nitrogen Status Signals after the 406 Formation of the C_4 FLs

407 Nitrogen assimilation by roots can be controlled by a number of signals representing the nitrogen status in the
408 shoots (Ruffel *et al.* 2008; Forde 2002). These signals include phytohormones such as auxin and cytokinin (Kiba
409 *et al.* 2011). Our results showed that several genes involved in the biosynthesis, transport, and biodegradation of
410 phytohormones were differentially expressed in the hypocotyls after formation of the FLs. Cytokinin signaling
411 increased after the establishment of C_4 photosynthesis. Shoot-derived cytokinin is a signal of nitrogen satiety in
412 well-supplied nitrogen conditions, suppressing the nitrogen uptake by roots (Kiba *et al.* 2011). Our findings
413 suggest that long-range cytokinin signaling can be a candidate pathway for controlling nitrogen uptake in C_4
414 plants. No particular cytokinin transporters for this shoot-to-root movement through the phloem has been
415 identified yet, but ENTs are likely involved (Liu, Zhao and Zhang 2019). Type-B ARR is the positive regulator
416 of cytokinin signaling (Argyros *et al.* 2008) and type-A ARR is the negative regulator of cytokinin signaling (To
417 *et al.* 2004) which have their corresponding transcripts (AT1G67710 and AT3G57040) up- and down-regulated,
418 respectively, in the hypocotyl B.

419 Due to its role in lateral root initiation, auxin has long been known as a shoot-to-root nitrogen signal (Forde 2002;
420 Fukaki and Tasaka 2009). In the C_4 crop maize, auxin concentration in phloem exudates decreases under high
421 nitrate concentrations (Tian *et al.* 2008). In the same line, our data showed that cell-to-cell auxin transporters,
422 responsible for auxin's long-distance movement and an enzyme catalyzing the rate-limiting step in auxin
423 biosynthesis, were down-regulated in hypocotyls B. In contrast, the intracellular auxin transporters that modulate
424 the nuclear abundance of auxin by transporting auxin into the ER lumen (Sauer and Kleine-Vehn 2019) were up-

425 regulated. These findings imply that long-distance movement of auxin is reduced in hypocotyls after C_4 leaf
426 formation. At the same time, the NRT1.1 transporter becomes down-regulated in hypocotyls B. As a dual-affinity
427 transporter, NRT1.1 acts as a nitrate sensor that regulates the expression level of genes involved in nitrate transport
428 (Sun and Zheng 2015). It is located in roots, vascular cells, and shoots and displays an auxin-responsive activity.
429 The reduced expression in hypocotyl B is consistent with other findings in this study, implying a general reduction
430 of auxin content, either derived from leaves or the hypocotyl itself, in the hypocotyl B. Furthermore, NRT1.1 has
431 a significant role in the nitrogen uptake in roots affected by shoot-derived signals. Thus, its lower expression in
432 roots after formation of the first leaves (Fig. 8(c)) may be a response to a decrease in the nitrogen uptake by roots
433 after C_4 establishment. Other reports claim, however, that local increases of auxin biosynthesis and transport in
434 developing leaves is necessary for manifestation of C_4 key property of higher vein density (Huang *et al.* 2017).

435 A further mobile regulator mediating nitrogen assimilation in roots under nitrogen deficiency condition,
436 is CEP which has a shoot orientation from the roots. CEP receptor, like CEPR2, was down-regulated in hypocotyl
437 B (Fig. 8(d)), most likely due to the efficient use of nitrogen by C_4 plants. This likely reflects the reduced effect
438 of root-derived CEP signal after C_4 leave's formation. Indeed, this receptor implicates nitrogen uptake signaling
439 by enhancing the expression of NRT1(Tabata *et al.* 2014; Ohkubo *et al.* 2017). The observed lower NRT1
440 expression in roots after C_4 first leave's formation (Fig. 8(c)) is thus consistent with possible reduced root-derived
441 CEP. Notably, CEPR2 expression was higher in the cotyledon B (C_3) compared to the FLs (C_4) (Fig. 8(a)),
442 indicating a higher level of nitrogen consumption by C_3 cotyledons than by C_4 leaves.

443 Taken together, gene expression changes after emerging C_4 photosynthesis in the FLs indicate modulated
444 auxin and cytokinin metabolism and signaling alongside a reduced CEP signaling in hypocotyl B and FLs. This
445 supports the notion of an enhanced nitrogen use efficiency and reduction in total nitrogen requirement in C_4 plants
446 (Jobe *et al.* 2020).

447 Drought Resistance and Water Use Efficiency: Several Pathways involved in the High-
448 Temperature Resistance after the Formation of the C_4 FLs

449 Through different mechanisms, C_4 plants produce more efficiently than C_3 under higher temperatures. One
450 mechanism is preventing dehydration through stomatal closure. Stomatal closure under drought stress is regulated
451 by root-derived abscisic acid (Kuromori, Seo and Shinozaki 2018). Some studies claim that stomata of C_4 plants
452 are more sensitive to intercellular CO_2 concentration (Ci) compared to C_3 (Huxman and Monson 2003), and that
453 abscisic acid can increase this sensitivity (Dubbe, Farquhar and Raschke 1978). We observed that the expression

454 level of several abscisic acid influx genes (ABCG30, ABCG40) (Zhang *et al.* 2014; Kang *et al.* 2015) was up-
455 regulated in hypocotyls B compared to hypocotyls A (Fig. 6, Fig. 8(d)). Our finding for up-regulation of ABCG40
456 in C_4 leaves compared to C_3 cotyledons (Fig. 8(a)) is consistent with its functions in shoots as a root-derived-
457 abscisic acid importer and its essential role in stomatal closure (Kang *et al.* 2010). The differential regulation of
458 ABCG40 in roots (Fig. 8(d)) likely is due the interaction between abscisic acid and nitrate uptake (Harris and
459 Ondzighi-Assoume 2017). Moreover, studies on the amphibious *Eleocharis vivipara* have revealed the significant
460 role of abscisic acid and hormonal control in the manifestation of Kranz anatomy (Ueno 1998).

461 **Stress- and Light-Responsive Differentially expressed Mobile TFs in Hypocotyls are Possibly**
462 **Involved in the Formation of C_4 Unique Features**

463 Many of the TFs that are up-regulated in the hypocotyls after the formation of the FLs are implicated in the
464 regulatory networks controlling responses to the different plant development and growth conditions as well as
465 abiotic stresses. The appearance of C_4 leaves in *H. mollissima* Bunge, and other halophytes or xerohalophytes
466 switching chenopods is coincides with an increase in environmental temperature (Rudov *et al.* 2020).
467 Transcriptome analysis of C_3 cotyledons and C_4 leaves in *Salsola soda* demonstrated that 55 and 32 TFs were
468 increased and decreased in C_4 leaves compared to C_3 cotyledons, respectively (Lauterbach, Billakurthi et al. 2017).
469 Not surprisingly, a greater number of the up-regulated TFs in our study were stress-responsive, including NAC
470 (Shao, Wang and Tang, 2015), WRKY (Wang *et al.* 2018), and NF-Y (Zhao *et al.* 2017).

471 Among the differentially expressed TFs in hypocotyls before and after the formation of the C_4 FLs, SHR
472 and HY5 TFs are known to be mobile although at protein level (Dolan 2001; Chen *et al.* 2016). SHR is implicated
473 in modulating endodermis (known as bundle-sheath) differentiation in leaves and apparently plays a role in the
474 Kranz anatomy formation in maize (Slewinski *et al.* 2012). Moreover, Siadjeu et al. (Siadjeu, Lauterbach and
475 Kadereit 2021) who compared transcriptome data of C_3, C_2, and C_4 species from *Camphorosmeae*, found that,
476 BBX15, SHR, SCZ, and LBD41 are more expressed and co-regulated in the C_4 than C_3 species. Interestingly, out
477 of 38 differentially expressed Arabidopsis orthologous TFs in the comparative transcriptomic analysis between
478 Kranz (foliar leaf blade) and non-Kranz (husk leaf sheath) maize leaves, we identified four TFs that express more
479 in hypocotyl after C_4 leave's formation; including SHR (AT4G37650), BHLH96 (AT1G72210), GATA7
480 (AT4G36240) and WRKY12 (AT2G44745).

481 Most of the up-regulated TFs after C_4 manifestation belonged to C2H2 and bZIP families, including
482 HY5. HY5 is a master regulator of transcription (Gangappa and Botto 2016), a phloem-mediated shoot-to-root

483 signal for lateral root formation, and thus the carbon-nitrogen balance adjustment in Arabidopsis (Burko *et al.*
484 2020). HY5 mediates photomorphogenesis so that it is located downstream of phytochrome B, the sensor of light
485 and temperature (Legris *et al.* 2016). Thus, in C_4 plants where shoots are exposed to high light intensity and
486 temperature, and since the function of HY5 is conserved in many plants (Yamawaki *et al.* 2011; Huai, Jing and
487 Lin 2020), HY5 can be an appropriate candidate for synchronizing shoots and roots. Moreover, HY5 is one of the
488 light-responsive TFs essential in inhibiting hypocotyl elongation during seedling (Oyama, Shimura and Okada
489 1997). Therefore, HY5 is a shared regulator between several various pathways.

490 The mRNA of 12 differentially expressed TFs in the *H. mollissima* Bunge hypocotyls have cell-to-cell
491 mobility, according to the TAIR database (Table 1). We also predicted the probable cis-elements present in the
492 promoter region of their orthologous in *A. thaliana*. Several of the predicted cis-elements in the mobile TFs were
493 light- and stress-responsive (Additional file 10). This indicates that expression and transport of these TFs is
494 influenced by abiotic stresses. One of these TFs is WRKY40, an orthologue of which, ZmWRKY40, is a drought-
495 responsive gene in *Zea mays* (Wang *et al.* 2018). HSFA1e was more expressed in hypocotyl B, which is implicated
496 in the tolerance to heat shock stress via transcriptional regulation of HsfA2 function (Nishizawa-Yokoi *et al.*
497 2011). Overexpression of maize ZmHsf06 in Arabidopsis, improves drought-stress tolerance (H. Li *et al.* 2015).
498 The findings of this study pave the way for identifying possible regulators underlying the coordination of
499 developmental changes associated with functional C_4 photosynthesis. Also, by investigating a plant with a NAD-
500 ME subtype of C_4 photosynthesis our data fills the gap caused by previous studies solely concentrating on the
501 NADP-ME subtype of photosynthesis. Our data provides a valuable source for further functional genomics and
502 genetic studies to identify master regulators of C_4-related traits and engineering C_4 features into C_3 crops.

503 **Funding**

504 A.M.B-M gratefully acknowledges the financial support from the Iran National Science Foundation (INSF)
505 [funding reference number 95838484].

506 **Author Contribution**

507 MZ performed the experiments, analyzed data, and wrote the original draft. TR performed the microscopic
508 analysis and critically revised the manuscript. MRG analyzed data. AMB-M conceived and designed the research,
509 supervised the experiment, and critically revised the manuscript. All authors contributed to the article and
510 approved the submitted version.

Acknowledgment

We thank Stanislav Kopriva (University of Cologne) for the critical reading of the manuscript. We also would like to thank Alexander Rudov and Hossein Akhani (University of Tehran) for their support during seed collection.

Conflict of interest

The authors declare that the research was conducted in the absence of any commercial or financial relationships that could be construed as a potential conflict of interest.

Additional information

Supplementary Information

Supplementary file 1 Summary of A) sequencing information B) De novo transcriptome assembly results by Trinity

Supplementary file 2. The accession number of uploaded raw sequences to ??

Supplementary file 3. Active functional classes in the First leaves, hypocotyl A and hypocotyl B

Supplementary file 4. Abundance (total mean TPM) of C_4-related proteins and genes categorized in the CRP and NCRP signaling peptide groups

Supplementary file 5. Transcript abundance, statistics of differentially expressed genes, and their annotations.

Additional file 6. Venn diagram analysis of DEGs of two developmental *H.mollissima*'s hypocotyls and identified genes related to the hypocotyl developments in flax (Roach and Deyholos, 2008) and hemp (Behr *et al.* 2018) based on their assigned Arabidopsis ID

Supplementary file 7. List of the unique and shared genes compared to DEGs of two developmental *H.mollissima*'s hypocotyls and identified genes related to the hypocotyl developments in flax (Roach and Deyholos, 2008) and hemp (Behr *et al.* 2018) based on their assigned Arabidopsis ID.

Supplementary file 8. Functional analysis of the Cell signaling genes using Mapman

Supplementary file 9. Differentially transcription factor genes between hypocotyl A and hypocotyl B using PlantTFDB v5.0

535 **Supplementary file 10.** Cis-elements located upstream of orthologous transcription factor genes with mobile
536 mRNA in Arabidopsis

537 **Additional file 11** Validation of RNA-Seq results using quantitative RT-PCR (qRT-PCR)

538

539

540

541

542 **References:**

543 Akhani, H. *et al.* (2009) 'Does Bienertia cycloptera with the single-cell system of C4 photosynthesis exhibit a
544 seasonal pattern of δ13C values in nature similar to co-existing C4 Chenopodiaceae having the dual-cell (Kranz)
545 system?', *Photosynthesis Research*, 99(1), pp. 23–36.

546 Argyros, R.D. *et al.* (2008) 'Type B response regulators of Arabidopsis play key roles in cytokinin signaling and
547 plant development', *The Plant Cell*, 20(8), pp. 2102–2116.

548 Bartusch, K. and Melnyk, C.W. (2020) 'Insights into plant surgery: an overview of the multiple grafting
549 techniques for Arabidopsis Thaliana', *Frontiers in Plant Science*, p. 2000.

550 Behr, M. *et al.* (2018) 'Insights into the molecular regulation of monolignol-derived product biosynthesis in the
551 growing hemp hypocotyl', *BMC plant biology*, 18(1), pp. 1–18.

552 Bellstaedt, J. *et al.* (2019) 'A mobile auxin signal connects temperature sensing in cotyledons with growth
553 responses in hypocotyls', *Plant Physiology*, 180(2), pp. 757–766.

554 Burko, Y. *et al.* (2020) 'Local HY5 activity mediates hypocotyl growth and shoot-to-root communication', *Plant*
555 *communications*, 1(5), p. 100078.

556 Chen, X. *et al.* (2016) 'Shoot-to-root mobile transcription factor HY5 coordinates plant carbon and nitrogen
557 acquisition', *Current Biology*, 26(5), pp. 640–646.

558 Chomczynski, P. and Sacchi, N. (1987) 'Single-step method of RNA isolation by acid guanidinium thiocyanate-
559 phenol-chloroform extraction', *Analytical biochemistry*, 162(1), pp. 156–159.

560 Cui, H. (2021) 'Challenges and Approaches to Crop Improvement Through C3-to-C4 Engineering', *Frontiers in*
561 *Plant Science*, p. 1851.

562 Dolan, L. (2001) 'Root patterning: SHORT ROOT on the move', *Current biology*, 11(23), pp. R983–R985.

563 Dubbe, D.R., Farquhar, G.D. and Raschke, K. (1978) 'Effect of abscisic acid on the gain of the feedback loop
564 involving carbon dioxide and stomata', *Plant Physiology*, 62(3), pp. 413–417.

565 Fatima, Z. *et al.* (2018) 'Resource use efficiencies of C3 and C4 cereals under split nitrogen regimes', *Agronomy*,
566 8(5), p. 69.

567 Forde, B.G. (2002) 'Local and long-range signaling pathways regulating plant responses to nitrate', *Annual*
568 *Review of Plant Biology*, 53(1), pp. 203–224.

569 Freitag, H. and Kadereit, G. (2014) 'C3 and C4 leaf anatomy types in Camphorosmeae (Camphorosmoideae,
570 Chenopodiaceae)', *Plant Systematics and Evolution*, 300(4), pp. 665–687.

571 Fukaki, H. and Tasaka, M. (2009) 'Hormone interactions during lateral root formation', *Plant molecular biology*,
572 69(4), pp. 437–449.

573 Gangappa, S.N. and Botto, J.F. (2016) 'The multifaceted roles of HY5 in plant growth and development',
574 *Molecular plant*, 9(10), pp. 1353–1365.

575 Gerlich, S.C. *et al.* (2018) 'Sulfate metabolism in C4 Flaveria species is controlled by the root and connected to
576 serine biosynthesis', *Plant physiology*, 178(2), pp. 565–582.

577 Gowik, U. *et al.* (2011) 'Evolution of C4 photosynthesis in the genus Flaveria: how many and which genes does
578 it take to make C4?', *The Plant Cell*, 23(6), pp. 2087–2105.

579 Gowik, U. and Westhoff, P. (2011) 'The path from C3 to C4 photosynthesis', *Plant Physiology*, 155(1), pp. 56–
580 63.

581 Grabherr, M.G. *et al.* (2011) 'Full-length transcriptome assembly from RNA-Seq data without a reference
582 genome', *Nature biotechnology*, 29(7), pp. 644–652.

583 Haas, B. and Papanicolaou, A. (2016) 'TransDecoder (find coding regions within transcripts)', *Google Scholar*
584 [Preprint].

585 Harris, J.M. and Ondzighi-Assoume, C.A. (2017) 'Environmental nitrate signals through abscisic acid in the root
586 tip', *Plant signaling & behavior*, 12(1), p. e1273303.

587 Hibberd, J.M. and Covshoff, S. (2010) 'The regulation of gene expression required for C4 photosynthesis', *Annual*
588 *review of plant biology*, 61, pp. 181–207.

589 Hirner, A. *et al.* (2006) 'Arabidopsis LHT1 is a high-affinity transporter for cellular amino acid uptake in both
590 root epidermis and leaf mesophyll', *The Plant Cell*, 18(8), pp. 1931–1946.

591 Huai, J., Jing, Y. and Lin, R. (2020) 'Functional analysis of ZmCOP1 and ZmHY5 reveals conserved light
592 signaling mechanism in maize and Arabidopsis', *Physiologia Plantarum*, 169(3), pp. 369–379.

593 Huang, C.-F. *et al.* (2017) 'Elevated auxin biosynthesis and transport underlie high vein density in C4 leaves',
594 *Proceedings of the National Academy of Sciences*, 114(33), pp. E6884–E6891.

595 Huxman, T.E. and Monson, R.K. (2003) 'Stomatal responses of C3, C3-C4 and C4Flaveria species to light and
596 intercellular CO2 concentration: implications for the evolution of stomatal behaviour', *Plant, Cell & Environment*,
597 26(2), pp. 313–322.

598 Jobe, T.O. *et al.* (2020) 'Ensuring nutritious food under elevated CO2 conditions: A case for improved C4 crops',
599 *Frontiers in Plant Science*, 11, p. 1267.

600 Kang, J. *et al.* (2010) 'PDR-type ABC transporter mediates cellular uptake of the phytohormone abscisic acid',
601 *Proceedings of the National Academy of sciences*, 107(5), pp. 2355–2360.

602 Kang, J. *et al.* (2015) 'Abscisic acid transporters cooperate to control seed germination', *Nature communications*,
603 6(1), pp. 1–10.

604 Kiba, T. *et al.* (2011) 'Hormonal control of nitrogen acquisition: roles of auxin, abscisic acid, and cytokinin',
605 *Journal of experimental botany*, 62(4), pp. 1399–1409.

606 Ko, D. and Helariutta, Y. (2017) 'Shoot–root communication in flowering plants', *Current Biology*, 27(17), pp.
607 R973–R978.

608 Koenig, A.M. and Hoffmann-Benning, S. (2020) 'The interplay of phloem-mobile signals in plant development
609 and stress response', *Bioscience Reports*, 40(10).

610 Kuromori, T., Seo, M. and Shinozaki, K. (2018) 'ABA transport and plant water stress responses', *Trends in plant*
611 *science*, 23(6), pp. 513–522.

612 Lauterbach, M., Billakurthi, K., *et al.* (2017) 'C3 cotyledons are followed by C4 leaves: intra-individual
613 transcriptome analysis of Salsola soda (Chenopodiaceae)', *Journal of experimental botany*, 68(2), pp. 161–176.

614 Lauterbach, M., Schmidt, H., *et al.* (2017) 'De novo transcriptome assembly and comparison of C3, C3-C4, and
615 C4 species of tribe Salsoleae (Chenopodiaceae)', *Frontiers in plant science*, 8, p. 1939.

616 Legris, M. *et al.* (2016) 'Phytochrome B integrates light and temperature signals in Arabidopsis', *Science*,
617 354(6314), pp. 897–900.

618 Lescot, M. *et al.* (2002) 'PlantCARE, a database of plant cis-acting regulatory elements and a portal to tools for
619 in silico analysis of promoter sequences', *Nucleic acids research*, 30(1), pp. 325–327.

620 Li, B. and Dewey, C.N. (2011) 'RSEM: accurate transcript quantification from RNA-Seq data with or without a
621 reference genome', *BMC bioinformatics*, 12(1), pp. 1–16.

622 Li, H. *et al.* (2015) 'Expression of maize heat shock transcription factor gene ZmHsf06 enhances the
623 thermotolerance and drought-stress tolerance of transgenic Arabidopsis', *Functional Plant Biology*, 42(11), pp.
624 1080–1091.

625 Li, Y. *et al.* (2015) 'Developmental genetic mechanisms of C4 syndrome based on transcriptome analysis of C3
626 cotyledons and C4 assimilating shoots in Haloxylon ammodendron', *PLoS One*, 10(2), p. e0117175.

627 Liu, C.-J., Zhao, Y. and Zhang, K. (2019) 'Cytokinin transporters: multisite players in cytokinin homeostasis and
628 signal distribution', *Frontiers in Plant Science*, p. 693.

629 Livak, K.J. and Schmittgen, T.D. (2001) 'Analysis of relative gene expression data using real-time quantitative
630 PCR and the 2− ΔΔCT method', *methods*, 25(4), pp. 402–408.

631 Lohse, M. *et al.* (2014) *M ercator: a fast and simple web server for genome scale functional annotation of plant*
632 *sequence data*. Wiley Online Library.

633 McKown, A.D. and Dengler, N.G. (2007) 'Key innovations in the evolution of Kranz anatomy and C4 vein pattern
634 in Flaveria (Asteraceae)', *American journal of botany*, 94(3), pp. 382–399.

635 Nishizawa-Yokoi, A. *et al.* (2011) 'HsfA1d and HsfA1e involved in the transcriptional regulation of HsfA2
636 function as key regulators for the Hsf signaling network in response to environmental stress', *Plant and Cell*
637 *Physiology*, 52(5), pp. 933–945.

638 Ohkubo, Y. *et al.* (2017) 'Shoot-to-root mobile polypeptides involved in systemic regulation of nitrogen
639 acquisition', *Nature plants*, 3(4), pp. 1–6.

640 Oyama, T., Shimura, Y. and Okada, K. (1997) 'The Arabidopsis HY5 gene encodes a bZIP protein that regulates
641 stimulus-induced development of root and hypocotyl', *Genes & development*, 11(22), pp. 2983–2995.

642 Rao, X. and Dixon, R.A. (2016) 'The differences between NAD-ME and NADP-ME subtypes of C4
643 photosynthesis: more than decarboxylating enzymes', *Frontiers in plant science*, 7, p. 1525.

644 Reyna-Llorens, I. and Hibberd, J.M. (2017) 'Recruitment of pre-existing networks during the evolution of C4
645 photosynthesis', *Philosophical Transactions of the Royal Society B: Biological Sciences*, 372(1730), p. 20160386.

646 Roach, M.J. and Deyholos, M.K. (2008) 'Microarray analysis of developing flax hypocotyls identifies novel
647 transcripts correlated with specific stages of phloem fibre differentiation', *Annals of botany*, 102(3), pp. 317–330.

648 Robinson, M.D., McCarthy, D.J. and Smyth, G.K. (2010) 'edgeR: a Bioconductor package for differential
649 expression analysis of digital gene expression data', *Bioinformatics*, 26(1), pp. 139–140.

650 Rudov, A. *et al.* (2020) 'A review of C4 plants in southwest Asia: An ecological, geographical and taxonomical
651 analysis of a region with high diversity of C4 eudicots', *Frontiers in plant science*, 11, p. 1374.

652 Ruffel, S. *et al.* (2008) 'Systemic signaling of the plant nitrogen status triggers specific transcriptome responses
653 depending on the nitrogen source in Medicago truncatula', *Plant physiology*, 146(4), pp. 2020–2035.

654 Sadanandom, A. *et al.* (2012) 'The ubiquitin–proteasome system: central modifier of plant signalling', *New*
655 *Phytologist*, 196(1), pp. 13–28.

656 Sage, R.F. (2004) 'The evolution of C4 photosynthesis', *New phytologist*, 161(2), pp. 341–370.

657 Sauer, M. and Kleine-Vehn, J. (2019) 'PIN-FORMED and PIN-LIKES auxin transport facilitators', *Development*,
658 146(15), p. dev168088.

659 Schwacke, R. *et al.* (2019) 'MapMan4: a refined protein classification and annotation framework applicable to
660 multi-omics data analysis', *Molecular plant*, 12(6), pp. 879–892.

661 Shabala, S. *et al.* (2015) 'Root-to-shoot signalling: integration of diverse molecules, pathways and functions',
662 *Functional Plant Biology*, 43(2), pp. 87–104.

663 Shao, H., Wang, H. and Tang, X. (2015) 'NAC transcription factors in plant multiple abiotic stress responses:
664 progress and prospects', *Frontiers in plant science*, 6, p. 902.

665 Siadjeu, C., Lauterbach, M. and Kadereit, G. (2021) 'Insights into regulation of C2 and C4 photosynthesis in
666 Amaranthaceae/Chenopodiaceae using RNA-Seq', *International journal of molecular sciences*, 22(22), p. 12120.

667 Slewinski, T.L. *et al.* (2012) 'Scarecrow plays a role in establishing Kranz anatomy in maize leaves', *Plant and*
668 *Cell Physiology*, 53(12), pp. 2030–2037.

669 Slewinski, T.L. (2013) 'Using evolution as a guide to engineer Kranz-type C4 photosynthesis', *Frontiers in plant*
670 *science*, 4, p. 212.

671 Sun, J. and Zheng, N. (2015) 'Molecular mechanism underlying the plant NRT1. 1 dual-affinity nitrate
672 transporter', *Frontiers in Physiology*, 6, p. 386.

673 Tabata, R. *et al.* (2014) 'Perception of root-derived peptides by shoot LRR-RKs mediates systemic N-demand
674 signaling', *Science*, 346(6207), pp. 343–346.

675 Tian, Q. *et al.* (2008) 'Inhibition of maize root growth by high nitrate supply is correlated with reduced IAA levels
676 in roots', *Journal of plant physiology*, 165(9), pp. 942–951.

677 To, J.P.C. *et al.* (2004) 'Type-A Arabidopsis response regulators are partially redundant negative regulators of
678 cytokinin signaling', *The Plant Cell*, 16(3), pp. 658–671.

679 Ueno, O. (1998) 'Induction of Kranz anatomy and C4-like biochemical characteristics in a submerged amphibious
680 plant by abscisic acid', *The Plant Cell*, 10(4), pp. 571–583.

681 Usadel, B. *et al.* (2006) 'PageMan: an interactive ontology tool to generate, display, and annotate overview graphs
682 for profiling experiments', *BMC bioinformatics*, 7(1), pp. 1–8.

683 Vogan, P.J. and Sage, R.F. (2011) 'Water-use efficiency and nitrogen-use efficiency of C3-C4 intermediate
684 species of Flaveria Juss.(Asteraceae)', *Plant, cell & environment*, 34(9), pp. 1415–1430.

685 Wang, C.-T. *et al.* (2018) 'The maize WRKY transcription factor ZmWRKY40 confers drought resistance in
686 transgenic Arabidopsis', *International journal of molecular sciences*, 19(9), p. 2580.

687 Wang, L. *et al.* (2014) 'Comparative analyses of C4 and C3 photosynthesis in developing leaves of maize and
688 rice', *Nature biotechnology*, 32(11), pp. 1158–1165.

689 Wang, P., Vlad, D. and Langdale, J.A. (2016) 'Finding the genes to build C4 rice', *Current Opinion in Plant*
690 *Biology*, 31, pp. 44–50.

691 Xia, C. *et al.* (2018) 'Elucidation of the mechanisms of long-distance mRNA movement in a Nicotiana
692 benthamiana/tomato heterograft system', *Plant physiology*, 177(2), pp. 745–758.

693 Yamawaki, S. *et al.* (2011) 'Functional characterization of HY5 homolog genes involved in early light-signaling
694 in Physcomitrella patens', *Bioscience, biotechnology, and biochemistry*, 75(8), pp. 1533–1539.

695 Zhang, H. *et al.* (2014) 'A DTX/MATE-type transporter facilitates abscisic acid efflux and modulates ABA
696 sensitivity and drought tolerance in Arabidopsis', *Molecular plant*, 7(10), pp. 1522–1532.

697 Zhao, H. *et al.* (2017) 'The Arabidopsis thaliana nuclear factor Y transcription factors', *Frontiers in plant science*,
698 7, p. 2045.

699

700 **CAPTION of Table**:

701 **Table 1.** List of differentially expressed transcription factors between hypocotyl A and hypocotyl B with mobile

702 mRNAs based on TAIR database (https://www.arabidopsis.org/)

703

Arabidopsis ID	Transcription factor name	Transcription factor family	Log_2FC	FDR
AT3G10500	NAC053	NAC	10/19	7/19E-05
AT1G09770	CDC5	MYB_related	9/78	0/001280562
AT3G02990	HSFA1E	HSF	3/16	2/80E-05
AT1G69490	NAP	NAC	2/43	6/08E-06
AT1G21450	SCL1	GRAS	2/03	7/52E-10
AT1G80840	WRKY40	WRKY	1/32	2/32E-12
AT4G37790	HAT22	HD-ZIP	1/55	8/04E-06
AT5G47390	MYBH	MYB_related	1/52	1/21E-09
AT5G62020	HSFB2A	HSF	-1/84	2/75E-06
AT5G60690	REV	HD-ZIP	-3/12	0/030388143
AT5G59570	BOA	G2-like	-4/08	0/013424766
AT1G01720	ATAF1	NAC	-11/88	2/42E-21

CAPTION of Figures:

Fig. 1 Sampled tissues from *H. mollissima* Bunge in the current study a) Series A b) Series B

Fig. 2 Leaf and cotyledon cross-sections of *H. mollissima* Bunge a) Cross-section of the cotyledon (C_3), b) Cross-section of the entire leaf (C_4, Salsoloid type Kranz anatomy), and c) close-up of the leaf Kranz anatomy

Abbreviations: E, Epidermis; PM, palisade mesophyll; KC, Kranz cell; PVB, peripheral vascular bundle, MV, mid-vein, WS, water-storage tissue; AS, air space; CH, chlorenchyma. Bars = 100 µm (a, b), 25 µm (c)

Fig. 3 PCA analysis which explains 91.09% of the total variation. Principal component analysis of the read counts separated the samples based on the tissue type and indicated the consistency and validation of our normalized data

713 **Fig. 4** a) Active functional classes of each sample according to all percentages of all transcripts belonged to
714 Mapman categories **b)** Relative transcript abundance of C_4 cycle proteins: most C_4 proteins are more expressed in
715 leaves than in hypocotyls. Beta-carbonic anhydrase (BCA3), PEP carboxylase1 (PEPC1), pyruvate
716 orthophosphate dikinase (PPdK), aspartate aminotransferase (Asp-AT), alanine aminotransferase (Ala-AT),
717 NAD-dependent malic enzyme (NAD-ME), NADP-dependent malic enzyme (NADP-ME), Triosephosphate
718 translocator (TPT), Pyrophosphatase (PPase6), pyruvate orthophosphate dikinase related protein1 (PPdK-RP1),
719 PEP/phosphate translocator (PPT2), Bile acid:sodium symporter family protein (BASS4), Bile acid:sodium
720 symporter family protein (BASS2), Adenosine monophosphate kinase (AMK2), Dicarboxylate translocator1
721 (Dit1), phosphoenolpyruvate carboxykinase (PEPC-K)

722 **Fig. 5** Overrepresentation analysis of up- and down-regulated genes in pairwise comparison of hypocotyl B vs.
723 hypocotyl A within functional gene classes defined by MapMan bins (MapMan, v3.6, available online at
724 https://www.plabipd.de/portal/mercator4) in Pageman software. Fisher's exact test, followed by the Benjamini
725 Hochberg correction and cut-off value one, was used for functional enrichment of DEGs between three binary
726 comparisons

727 Blue, up- or downregulated genes are significantly overrepresented; red, up- or downregulated genes are
728 significantly underrepresented

729 **Fig. 6** "Cell signaling" using MapMan. Visualization of transcriptional changes in genes involved in the various
730 signaling pathways (FDR<0.05, log2FC>1.5 <-1.5) at hypocotyl B Vs. hypocotyl A (DEGs encoding
731 phytohormone synthesizing and degrading enzymes, transporter ("Phytohormone action bin" and "Solute
732 transporter"), and different signal transduction pathways ("Multi-process regulation. Calcium-dependent
733 signalling", "Protein modification. Protein kinase" and "Redox hemoestasis" bins))**;** Red, down-regulated gene,
734 and green, up-regulated genes

735 **Fig. 7** Relative transcript abundance of transcripts associated with a) CRP peptide activities b) NCRP peptide
736 activities

737 **Fig. 8** RT-qPCR analysis of selected genes in the tissues of interest a) (CotA, CotB Vs, FL) b) CotB Vs. CotA c)
738 RootB Vs. RootA d) Hypocotyl BVs. Hypocotyl A

739

740

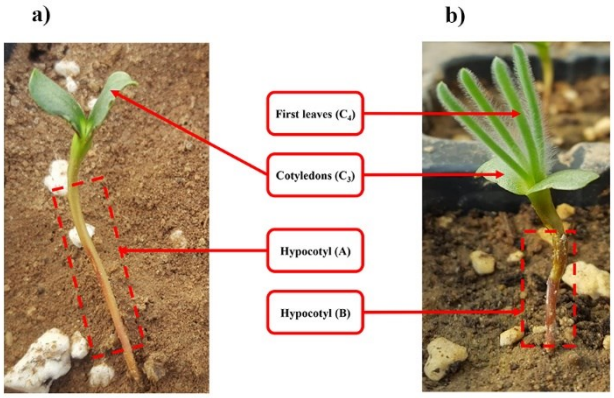
a)
b)
First leaves (C_4)
Cotyledons (C_3)
Hypocotyl (A)
Hypocotyl (B)

Fig. 1

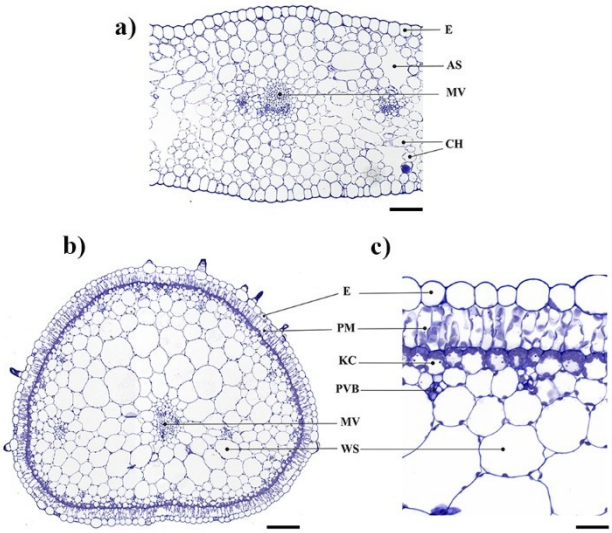
a)
E
AS
MV
CH
b)
c)
E
PM
KC
PVB
MV
WS

Fig. 2

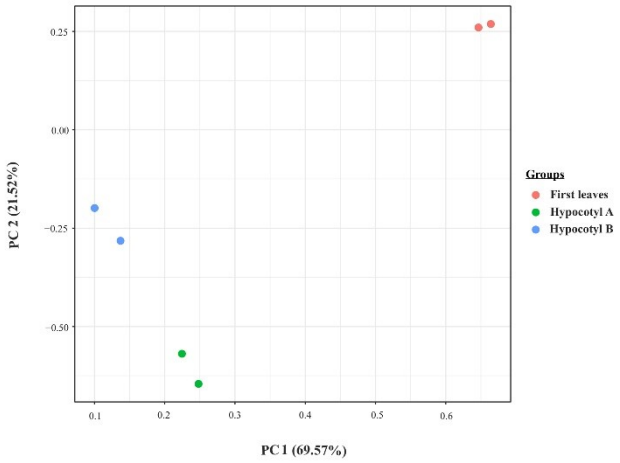
0.25
0.00
−0.25
−0.50
PC 2 (21.52%)
0.1
0.2
0.3
0.4
0.5
0.6
PC 1 (69.57%)
Groups
First leaves
Hypocotyl A
Hypocotyl B

Fig. 3

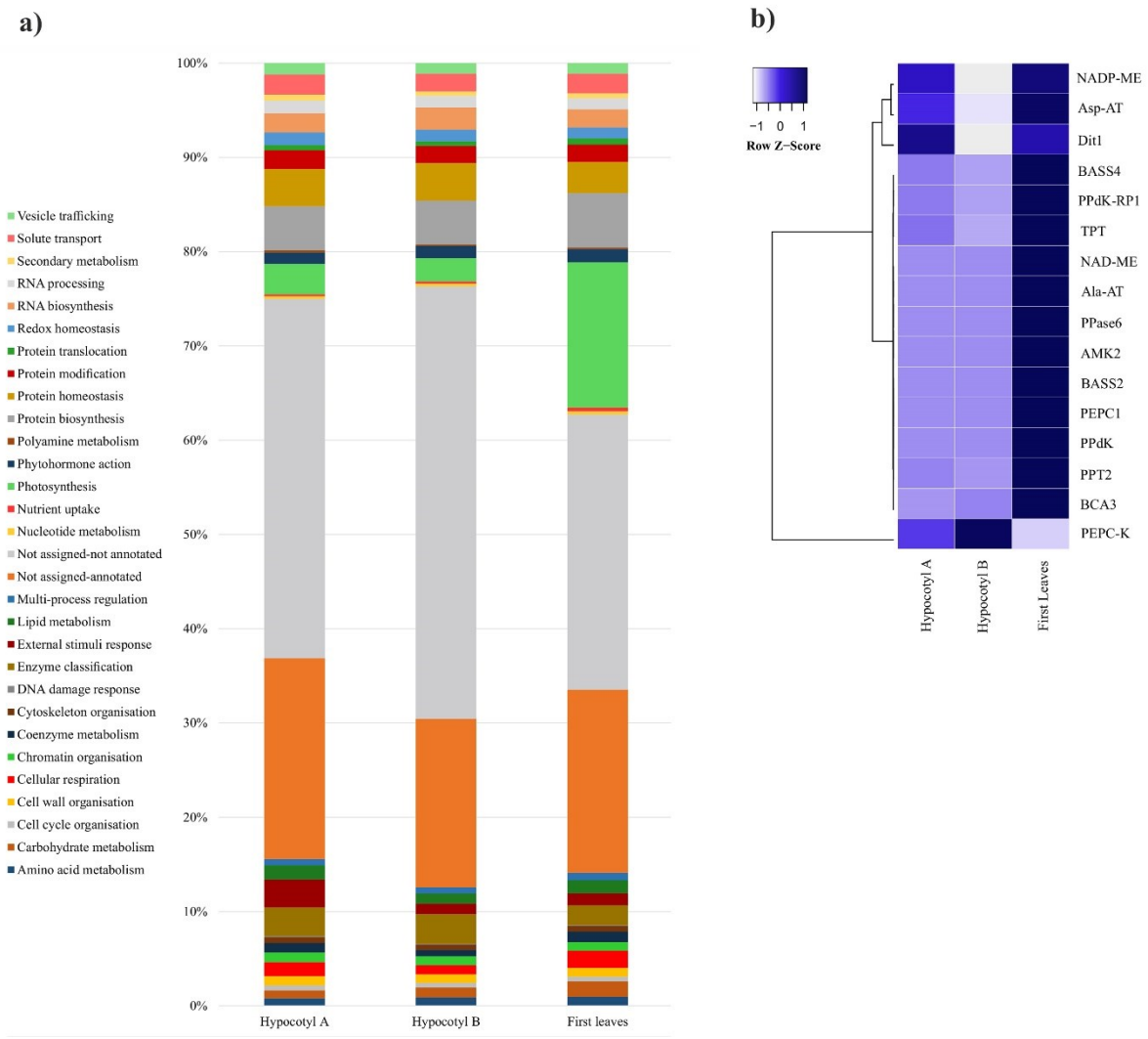
a)
b)
100%
90%
80%
70%
60%
50%
40%
30%
20%
10%
0%
Hypocotyl A
Hypocotyl B
First leaves
Vesicle trafficking
Solute transport
Secondary metabolism
RNA processing
RNA biosynthesis
Redox homeostasis
Protein translocation
Protein modification
Protein homeostasis
Protein biosynthesis
Polyamine metabolism
Phytohormone action
Photosynthesis
Nutrient uptake
Nucleotide metabolism
Not assigned-not annotated
Not assigned-annotated
Multi-process regulation
Lipid metabolism
External stimuli response
Enzyme classification
DNA damage response
Cytoskeleton organisation
Coenzyme metabolism
Chromatin organisation
Cellular respiration
Cell wall organisation
Cell cycle organisation
Carbohydrate metabolism
Amino acid metabolism
−1 0 1
Row Z−Score
NADP-ME
Asp-AT
Dit1
BASS4
PPdK-RP1
TPT
NAD-ME
Ala-AT
PPase6
AMK2
BASS2
PEPC1
PPdK
PPT2
BCA3
PEPC-K
Hypocotyl A
Hypocotyl B
First Leaves

Fig. 4

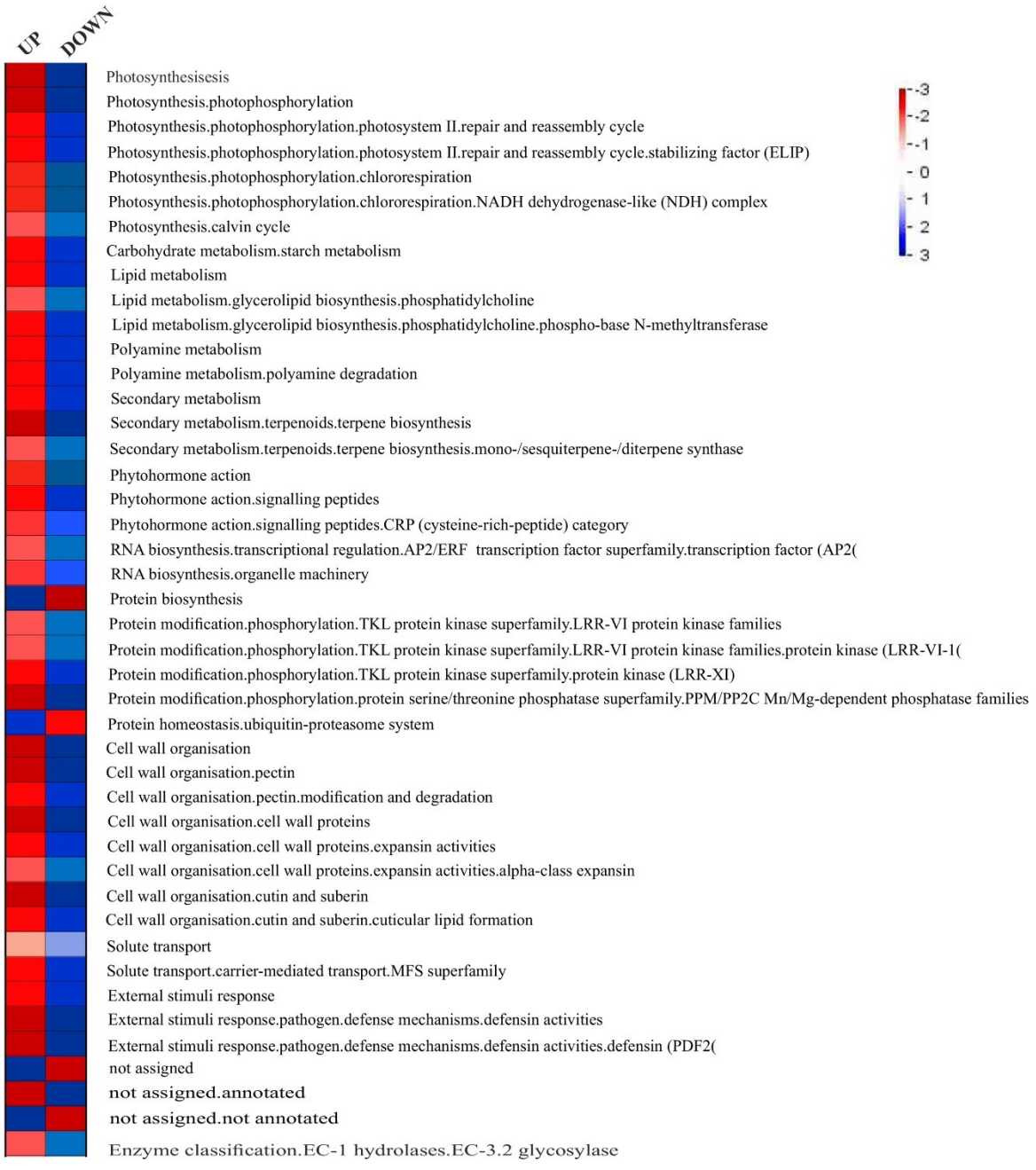
UP
DOWN
Photosynthesisesis
Photosynthesis.photophosphorylation
Photosynthesis.photophosphorylation.photosystem II.repair and reassembly cycle
Photosynthesis.photophosphorylation.photosystem II.repair and reassembly cycle.stabilizing factor (ELIP)
Photosynthesis.photophosphorylation.chlororespiration
Photosynthesis.photophosphorylation.chlororespiration.NADH dehydrogenase-like (NDH) complex
Photosynthesis.calvin cycle
Carbohydrate metabolism.starch metabolism
Lipid metabolism
Lipid metabolism.glycerolipid biosynthesis.phosphatidylcholine
Lipid metabolism.glycerolipid biosynthesis.phosphatidylcholine.phospho-base N-methyltransferase
Polyamine metabolism
Polyamine metabolism.polyamine degradation
Secondary metabolism
Secondary metabolism.terpenoids.terpene biosynthesis
Secondary metabolism.terpenoids.terpene biosynthesis.mono-/sesquiterpene-/diterpene synthase
Phytohormone action
Phytohormone action.signalling peptides
Phytohormone action.signalling peptides.CRP (cysteine-rich-peptide) category
RNA biosynthesis.transcriptional regulation.AP2/ERF transcription factor superfamily.transcription factor (AP2(
RNA biosynthesis.organelle machinery
Protein biosynthesis
Protein modification.phosphorylation.TKL protein kinase superfamily.LRR-VI protein kinase families
Protein modification.phosphorylation.TKL protein kinase superfamily.LRR-VI protein kinase families.protein kinase (LRR-VI-1(
Protein modification.phosphorylation.TKL protein kinase superfamily.protein kinase (LRR-XI)
Protein modification.phosphorylation.protein serine/threonine phosphatase superfamily.PPM/PP2C Mn/Mg-dependent phosphatase families
Protein homeostasis.ubiquitin-proteasome system
Cell wall organisation
Cell wall organisation.pectin
Cell wall organisation.pectin.modification and degradation
Cell wall organisation.cell wall proteins
Cell wall organisation.cell wall proteins.expansin activities
Cell wall organisation.cell wall proteins.expansin activities.alpha-class expansin
Cell wall organisation.cutin and suberin
Cell wall organisation.cutin and suberin.cuticular lipid formation
Solute transport
Solute transport.carrier-mediated transport.MFS superfamily
External stimuli response
External stimuli response.pathogen.defense mechanisms.defensin activities
External stimuli response.pathogen.defense mechanisms.defensin activities.defensin (PDF2(
not assigned
not assigned.annotated
not assigned.not annotated
Enzyme classification.EC-1 hydrolases.EC-3.2 glycosylase
-3
-2
-1
0
1
2
3

Fig. 5

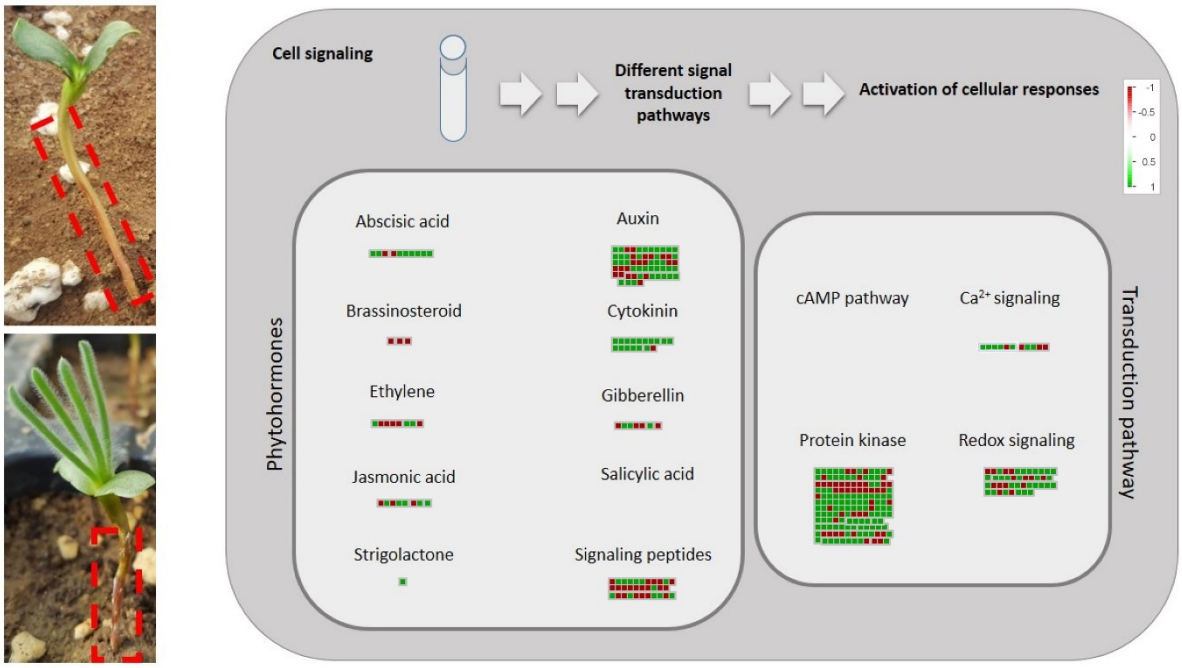
Cell signaling
Different signal transduction pathways
Activation of cellular responses
-1
-0.5
0
0.5
1
Phytohormones
Abscisic acid
Auxin
Brassinosteroid
Cytokinin
Ethylene
Gibberellin
Jasmonic acid
Salicylic acid
Strigolactone
Signaling peptides
Transduction pathway
cAMP pathway
Ca2+ signaling
Protein kinase
Redox signaling

Fig. 6

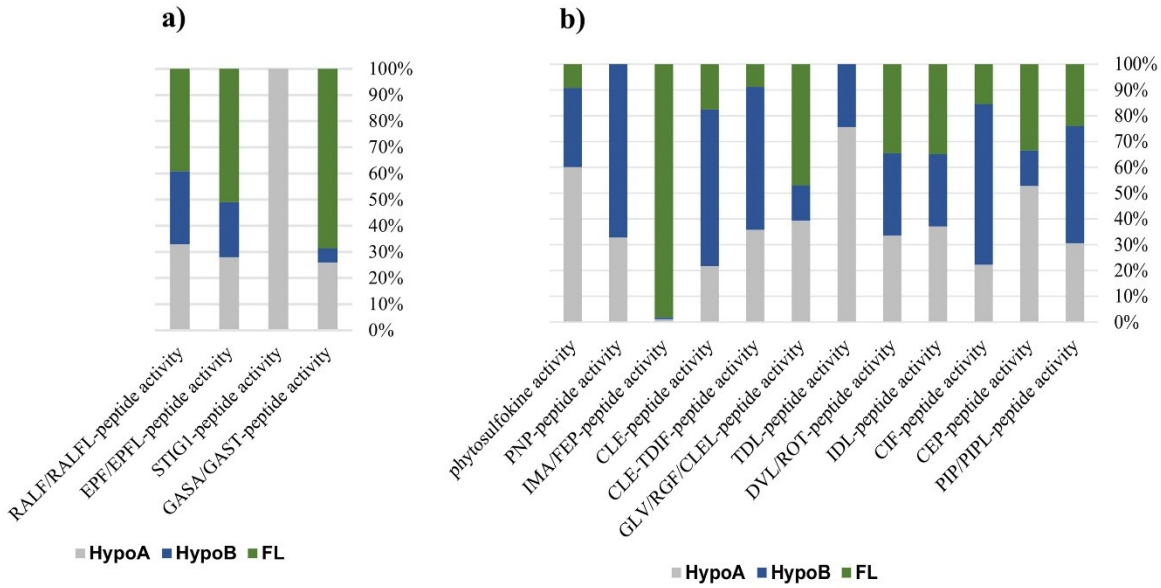
a)
100%
90%
80%
70%
60%
50%
40%
30%
20%
10%
0%
RALF/RALFL-peptide activity
EPF/EPFL-peptide activity
STIG1-peptide activity
GASA/GAST-peptide activity
HypoA
HypoB
FL
b)
100%
90%
80%
70%
60%
50%
40%
30%
20%
10%
0%
phytosulfokine activity
PNP-peptide activity
IMA/FEP-peptide activity
CLE-peptide activity
CLE-TDIF-peptide activity
GLV/RGF/CLEL-peptide activity
TDL-peptide activity
DVL/ROT-peptide activity
IDL-peptide activity
CIF-peptide activity
CEP-peptide activity
PIP/PIPL-peptide activity
HypoA
HypoB
FL

Fig. 7

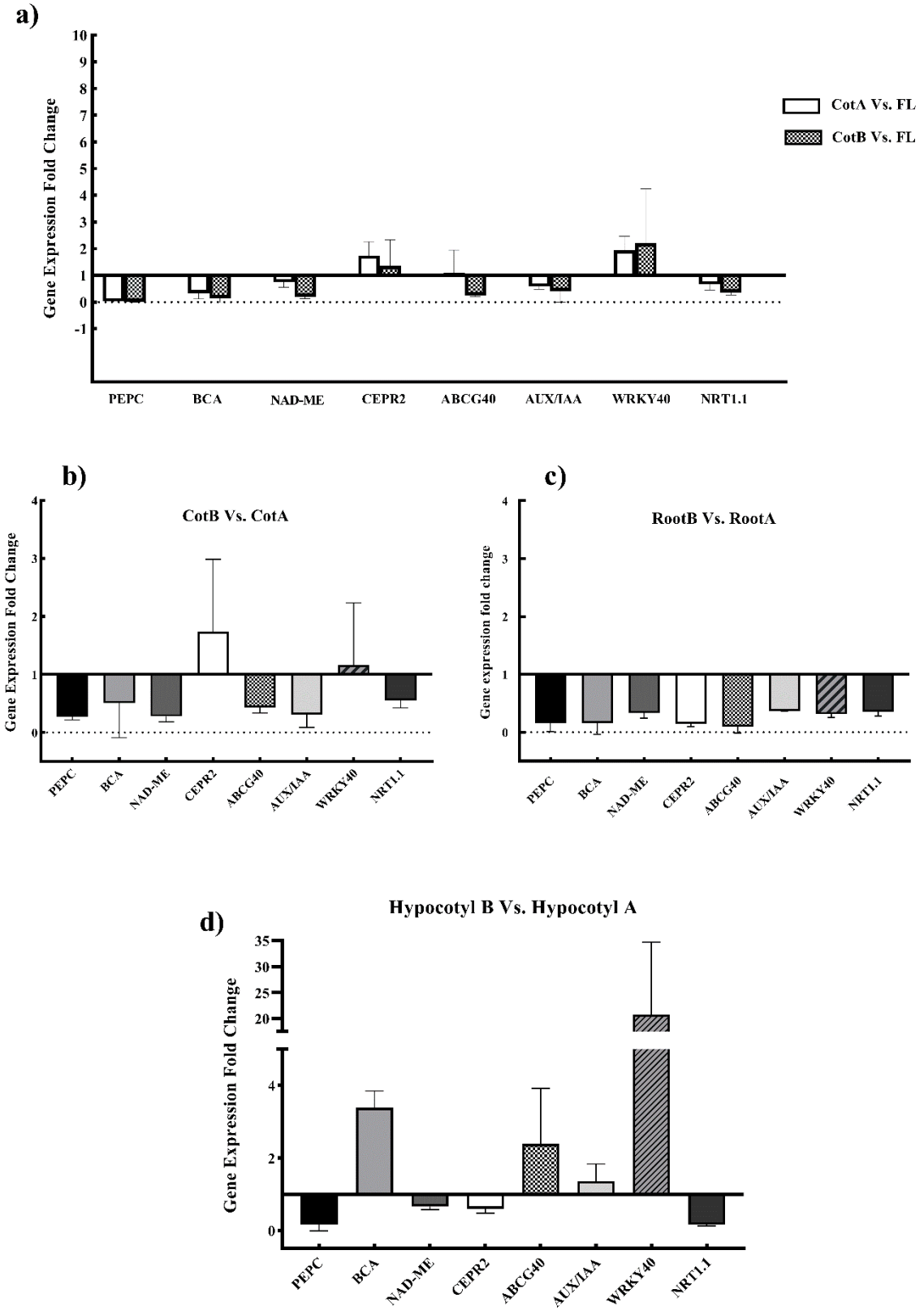
a)
Gene Expression Fold Change
CotA Vs. FL
CotB Vs. FL
PEPC
BCA
NAD-ME
CEPR2
ABCG40
AUX/IAA
WRKY40
NRT1.1
b)
CotB Vs. CotA
Gene Expression Fold Change
c)
RootB Vs. RootA
Gene expression fold change
d)
Hypocotyl B Vs. Hypocotyl A
Gene Expression Fold Change

767

768 **Fig. 8**